New Astronomy 35 (2015) 8–19

Contents lists available at ScienceDirect

New Astronomy

journal homepage: www.elsevier.com/locate/newast

Indian summer monsoon rainfall: Dancing with the tunes of the sun

K.M. Hiremath [a,*], Hegde Manjunath [a], Willie Soon [b]

[a] Indian Institute of Astrophysics, Bengaluru 560034, India
[b] Harvard-Smithsonian Center for Astrophysics, Cambridge, MA, USA

HIGHLIGHTS

- The purpose of this article is to find a physical linkage between solar activity and the summer monsoon rainfall.
- Hydrodynamical equations are used to derive an equation for the rate of precipitation.
- The equation for the rate of precipitation is similar to a forced harmonic oscillator.
- Forcing variables are cloud and rain water mixing ratios.
- Numerical solution captures very well the variability of Indian summer monsoon rainfall.

ARTICLE INFO

Article history:
Received 29 March 2014
Received in revised form 1 August 2014
Accepted 2 August 2014
Available online 19 August 2014

Communicated by P.S. Conti

Keywords:
Solar variability
Indian summer monsoon variability
Solar activity forcing on monsoon
Simulations of monsoon rainfall

ABSTRACT

There is strong statistical evidence that solar activity influences the Indian summer monsoon rainfall. To search for a physical link between the two, we consider the coupled cloud hydrodynamic equations, and derive an equation for the rate of precipitation that is similar to the equation of a forced harmonic oscillator, with cloud and rain water mixing ratios as forcing variables. Those internal forcing variables are parameterized in terms of the combined effect of external forcing as measured by sunspot and coronal hole activities with several well known solar periods (9, 13 and 27 days; 1.3, 5, 11 and 22 years). The equation is then numerically solved and the results show that the variability of the simulated rate of precipitation captures very well the actual variability of the Indian monsoon rainfall, yielding vital clues for a physical understanding that has so far eluded analyses based on statistical correlations alone. We also solved the precipitation equation by allowing for the effects of long-term variation of aerosols. We tentatively conclude that the net effects of aerosols variation are small, when compared to the solar factors, in terms of explaining the observed rainfall variability covering the full Indian monsoonal geographical domains.

1. Introduction

Indian agriculture and hence its thriving economy crucially depend upon both occurrence and intensity of the summer monsoon rainfall. It is remarkable to note that the Indian peninsular spans the range of subtropical latitudes more typical for desert environments (see Wu et al., 2009 for an in-depth perspective from atmospheric dynamics) than a motherland that sustains over 1 billion human population. Vagaries of floods and droughts related to extreme opposite ends of monsoonal rainfalls have caused immense loss of human lives, valuable cattle population and loss of agricultural outputs valued in billions of dollars. That is why a clear understanding of variability of Indian summer monsoon has remained a high priority for scientific research and breakthroughs.

It is generally accepted that summer monsoon rainfall is driven primarily by overall differential temperature gradient between the mainland and the sea that are ultimately heated and modulated by incoming sunlight. In fact, with century-long rainfall data recorded by instrumental rain gauges, a rather convincing set of analyses are suggesting that the varying sun's activity indeed influences the Indian monsoon rainfall (Bhalme and Mooley, 1980; Ananthakrishnan and Parthasarathy, 1984; Reddy et al., 1989; Kailas and Narasimha, 2000; Higginson et al., 2004; van Loon et al., 2004; Kerr, 2005; Badruddin et al., 2006; Hiremath, 2006a,b; Kodera et al., 2007; Perry, 2007; Claud et al., 2008; Hiremath, 2009a; Meehl et al., 2008; Meehl et al., 2009; Agnihotri et al., 2011; van Loon et al., 2012 and references therein). Our sun's influence on the Indian monsoon rainfall, especially on multidecadal to centennial timescales, can also be studied and deduced from a variety of paleoclimatic records (Nigam et al., 1995; Neff et al., 2001; Agnihotri et al., 2002; Agnihotri and

* Corresponding author.
E-mail address: hiremath@iiap.res.in (K.M. Hiremath).

http://dx.doi.org/10.1016/j.newast.2014.08.002
1384-1076/

Dutta, 2003; Higginson et al., 2004; Gupta et al., 2005; Tiwari et al., 2005; Wang et al., 2005; Thamban et al., 2007; Agnihotri et al., 2011). The general topic of solar forcing on Earth's climate has been recently reviewed by Gray et al. (2010); Soon and Legates (2013); Soon et al. (2014) and references therein.

Although sun's radiant energy is considered to be the main cause for the genesis of monsoon winds and the seasonal (i.e., the wet monsoonal versus dry non-monsoonal seasons) reversal of near-surface wind flows, that are sustained by the differential heatings of land and ocean masses, presently it is not understood how the sun's energy outputs are linked with the Indian summer monsoon rainfall changes from decade-to-decade nor even from year-to-year. We interpret a plausible influence of the magnetic sun on the summer monsoon rainfall as follows. Radiant energy by sun received by the ocean and land masses, either locally within the Indian ocean and subcontinent or remotely elsewhere, controls the amount of atmospheric water vapor that is ultimately connected to precipitation-and-cloud fields. If our proposed scenario is reasonable (see the work of Lim et al. (2006) for a similar proposal for the key role of atmospheric water vapor for the solar-activity-induced decadal variability over tropical Atlantic), owing to quasi-periodic solar activity, water vapor in the Earth's atmosphere might vary periodically in response to the different sun-originated periodic activities. As a consequence, it is therefore not too surprising to find hints of several quasi-periodic signals from time-series analyses of Indian summer monsoon rainfall records (Vines, 1986; Kailas and Narasimha, 2000; Hiremath and Mandi, 2004; Ma et al., 2007; Hiremath, 2009a; Agnihotri et al., 2011) and its proxies (Yadava and Ramesh, 2007; Ramesh et al., 2010; Knudsen et al., 2012; Maitra et al., 2014) that correspond to those natural periods from the sun's activity.

It is equally clear there may be various non-solar factors of the Indian monsoonal rainfall variability, both deterministic and stochastic, that may contribute to the phenomenon we are attempting to study. But we shall prescribe an underlying solar-Indian monsoon relation through a parametric modeling of the physically relevant solar activity and monsoonal rainfall quantities in order to see how well we can emulate the measured Indian summer monsoonal rainfall from 1871 through 2005. If the outcome is negative, then one can suggest that the proposed hypothesis for solar-monsoon rainfall correlation can be strongly rejected. In contrast, if the simulation may turn out to be positive, then one may at least diagnose and identify some of the relevant physical quantities involved. We proffer such an avenue of parametric modeling approach in order to reach the ultimate physical understanding of any solar-monsoonal rainfall connection. It is important to acknowledge that our proposed minimal parametric modeling approach (as discussed in more details below) is partly motivated by and is consistent with the findings of van Loon et al. (2012) where those authors found that the net solar radiation and latent heat flux indeed control the near-surface energy budget in the relatively cloud-free part of the southern Indian ocean (0–15°S; 60–100°E) on decadal solar oscillation timescale. Our pursuit of solar-Indian monsoon relation should ultimately be sought in terms of how solar activity may modulate the linkages and interconnection among the southern Indian Ocean anticyclones, Indian Ocean Dipole and El-Nino-Southern Oscillation from the perspective of coupled atmosphere–ocean dynamics as sketched by previous studies (Gadgil et al., 2004; Kodera et al., 2007; Claud et al., 2008; Agnihotri et al., 2011).

It is well known that sunspot activity is the most obvious manifestation of the solar magnetic phenomena that in turn is related to a host of other solar magnetic features and dynamic phenomena including the solar faculae and plages, solar flares, coronal mass ejections, etc. Recent observations from the satellites, especially in the high energy X-ray and UV windows, brought the hitherto less well known solar magnetic disturbing regions, *viz.*, coronal holes (Wang, 2009; Cranmer, 2009) as also one of the prominent solar activity phenomena. The solar coronal hole (CH) is now identified as the source of fast solar wind that creates disturbances in the Earth's atmosphere (Soon et al., 2000; Sykora et al., 2000; Lei et al., 2008; Choi et al., 2009; Shugai et al., 2009; Sojka et al., 2009; Ram et al., 2010; Verbanac et al., 2011; Mannucci et al., 2012; Hiremath and Hegde, 2013). During a particular solar activity cycle, activity of the coronal holes occur in advance and hence there is a phase lag (Bravo and Stewart, 1997) for the occurrence of sunspot activity. In terms of spatial domain, sunspot variability is primary a phenomenon around middle to low solar latitudes while the coronal hole activity is largely a phenomenon covering the polar and mid-latitude regions of the sun. Thus we suspect that the Earth probably receives the combined effect of sunspot and coronal hole disturbances and hence the consideration of energy outputs from the sun must include both these effects. It may be pointed out that the physical motivation for including coronal hole indices (area or other derived properties including sources of fast solar winds) for a sun-climate study can be found in the earlier statistical correlation study (Soon et al., 2000).

The sun is a variable star whose activity and hence its energy outputs vary on time scales of few minutes to months, years to decades and perhaps even on century time scales. Recent observations of a persistent 5-min global oscillations – due to pressure gradient variations in the interior of the sun – yielded rich dividends on the internal dynamic, thermal and magnetic field structures of the sun. Other manifestations of sun's periodic oscillations are: 9, 13 and 27 days; 1.3, 5, 11 and 22 years. Although physics of 5-min oscillations of the sun is well understood (Hiremath, 2013), however, the physics for the rest of the longer period oscillations is not understood completely (Hiremath, 2010).

Presently, there are indeed many studies focusing on the simulations and predictions of Indian summer monsoon rainfall that mainly concentrate on the local micro and macro physics as well as several locally and remotely inter-connected circulation phenomena of the coupled ocean–atmosphere. Such studies are conducted using the most sophisticated general circulation models (Kripalani et al., 2007; Preethi et al., 2010; Sabade et al., 2011; Rajeevan et al., 2012; DelSole and Shukla, 2012; Gadgil and Srinivasan, 2012; Krishnamurty and Shukla, 2012; Krishnan et al., 2012) with a range of successes and unsatisfactory outcomes in terms of a comprehensive understanding of all co-varying factors for the Indian monsoon rainfall variations. Among the currently unresolved issues is the lack of long-term trend in the measured Indian summer monsoon rainfall when compared to some of the simulated series as forced by increased atmospheric CO_2 (Kripalani et al., 2007; Sabade et al., 2011). This is why we consider our present approach is an important alternative avenue for scientific research with the ultimate aim of learning more about both the nature of solar magnetic variations and its associated physical linkages to the underlying Indian monsoon rainfall variability.

In the present study, from the coupled cloud hydrodynamic equations, we derive an equation of rate of precipitation that is similar to equation of a forced harmonic oscillator with cloud and rain water mixing ratios as the forcing variables. These forcing variables in turn are parameterized in terms of combined effect of external forcing due to sunspot and coronal hole activities with the well known solar periodicities. Next the derived equation for the rate of precipitation is numerically solved and compared with the observed Indian summer monsoon rainfall activity. We find that the solution of precipitation variability matches very well with the observed Indian rainfall variability yielding insights regarding a physical link between the Indian summer monsoon rainfall and the sun's activity. We also evaluated the effects of aerosol forcing on simulated Indian monsoon rainfalls, although this effort needs

further more detailed and in-depth handling in terms of the physical and chemical parameterization of the aerosols effects. This manuscript is organized as follows. In Section 2, we derive equation for the rate of precipitation and present description of the same in Section 2.1. The solutions and results are shown in Section 3, further discussion and checking of our assumptions as well as the research conclusions are presented in Section 4.

2. Derivation of the equation for the rate of precipitation

We propose a novel method for studying and examining sun-Indian monsoon rainfall connection. Owing to the shortness of available instrumental rainfall data, we shall restrict all our discussion in variations and changes on interannual to decadal timescales. We begin by deriving a single ordinary differential equation for describing the rate of precipitation from the following set of coupled nonlinear equations for cloud-and-rain-related hydrodynamics. Assuming that cloud is a structure that is mainly distributed vertically along the z axis in the Cartesian geometry, the nonlinear coupled hydrodynamic partial differential equations (Srivastava, 1967; Rogers, 1979) that are relevant to Earth's atmosphere are considered. As the structure of summer monsoon clouds is not yet completely understood (Johnson et al., 1987), the terminology "cloud" used in this study simply means *precipitating clouds*. For the present study relevant hydrodynamic equations are

$$\frac{\partial U}{\partial t} = -U\frac{\partial U}{\partial z} + gB - g(W+R), \tag{1}$$

$$\frac{\partial X}{\partial t} = -U\frac{\partial X}{\partial z} + E, \tag{2}$$

$$\frac{\partial W}{\partial t} = -U\frac{\partial W}{\partial z} - E_1 - P, \tag{3}$$

$$\frac{\partial R}{\partial t} = -U\frac{\partial R}{\partial z} - \frac{1}{\rho}\frac{\partial}{\partial z}(\rho RV) - E_2 + P, \tag{4}$$

where P describes the rate of production of rain from the cloud by spontaneous coalescence and by accretion, t is time variable, ρ is density, V is the effective fall velocity, X is water vapor mixing ratio, U is the vertical velocity, E_1 is the term that describes cloud evaporation or condensation, E_2 is a term that describes the rate of evaporation of rain, $E = E_1 + E_2, g$ is acceleration due to gravity, the dimensionless temperature ratio, $B = (T - T')/T'$ (with $T(z,t)$ is the temperature of the cloud and $T'(z,t)$ is the ambient temperature) and, the terms R and W represent cloud water and rain water mixing ratios, respectively. Basically these equations are representatives of momentum equation for different parameters. In Eq. (1), the third term on the right hand side of equation represents reduction in buoyancy due to weight of condensed water. Without this term, this equation is momentum equation with buoyant parcel of matter. Although different symbols (such as U, V, etc., that describe physical terms in the above equations) differ with the physical terms commonly used in meteorology, for the sake of our convenience, we retain the terms as described in the previous studies (Srivastava, 1967; Rogers, 1979). Subtracting Eq. (3) from (4) we get,

$$\frac{\partial}{\partial t}(R-W) = U\frac{\partial}{\partial z}(W-R) - \frac{1}{\rho}\frac{\partial}{\partial z}(\rho RV) + (E_1 - E_2) + 2P. \tag{5}$$

Differentiating the above equation with respect to time and rearranging the terms, we get the following equation:

$$2\frac{\partial P}{\partial t} = \frac{\partial}{\partial t}(E_2 - E_1) + \frac{1}{\rho}\frac{\partial}{\partial z}\left[\rho\left(R\frac{\partial V}{\partial t} + V\frac{\partial R}{\partial t}\right)\right] + \frac{\partial U}{\partial t}\frac{\partial}{\partial z}(R-W) + U\frac{\partial}{\partial z}\left[\frac{\partial R}{\partial t} - \frac{\partial W}{\partial t}\right] + \frac{\partial^2}{\partial t^2}(R-W). \tag{6}$$

Collecting all the P terms on one side and using Eqs. (1), (3) and (4), we get

$$\begin{aligned} 2\frac{\partial P}{\partial t} - \frac{1}{\rho}\frac{\partial}{\partial z}(\rho VP) - 2U\frac{\partial P}{\partial z} &= \frac{\partial}{\partial t}(E_2 - E_1) \\ &+ \frac{1}{\rho}\frac{\partial}{\partial z}\left[\rho\left\{R\frac{\partial V}{\partial t} + V\left(-U\frac{\partial R}{\partial z} - \frac{1}{\rho}\frac{\partial}{\partial z}(\rho RV) - E_2\right)\right\}\right] \\ &+ \left[-U\frac{\partial U}{\partial z} + gB - g(W+R)\right]\frac{\partial}{\partial z}(R-W) \\ &+ U\frac{\partial}{\partial z}\left[U\frac{\partial}{\partial z}(W-R) - \frac{1}{\rho}\frac{\partial}{\partial z}(\rho RV) + (E_1 - E_2)\right] \\ &+ \frac{\partial^2}{\partial t^2}(R-W). \end{aligned}$$

Because the above partial differential equation is very complicated and we are interested in the temporal variations that are longer than the cloud's life time ($\sim$ few minutes to one hour), the following assumptions are made: (i) E_1 and E_2 are independent of time that is greater than the cloud's life time, (ii) density of the cloud is constant with respect to time and vertical z coordinate and, (iii) except for P (which is assumed to vary as $P(z,t) = P(t)e^{-z}$, where z is a vertical variable), the parameters R, U, V and W are independent of z but are function of time. For the validity of assumption (i), although the rates of formation of cloud water and rainfall change significantly on short time scales of $\sim$ minutes to hours, but we note that our simulations are for time scales longer than a day which is also greater than cloud's life time. This is why we feel it is reasonable to assume that these two parameters are independent on longer time scales of days to months and years in our simulations.

The reasons regarding the validity of the assumption that density of the cloud is independent of time is given in Section 3.1 below. It seems also reasonable to assume the constancy of cloud's density structure with the altitude because the observational inference of density structure of clouds in monsoonal weather and climate regimes (Prabha et al., 2011) indeed shows relatively constant variation as a function of altitude.

The assumption that the terms R, U, V, and W are independent of altitude is not strictly correct when the cloud is actively developing. On the other hand, we presumed that first cloud develops and reaches a steady state. Hence, our simulation is valid only when the cloud system/entity reaches a steady state regime. Moreover, in the following section, from the numerical simulations we find uniquely that unless the cloud thickness is of $\sim$1 km, the simulated rainfall does not matches the Indian monsoon rainfall very well. Interestingly, it can be noted that the thickness ($\sim$1 km) of the cloud used in the simulations is very small when compared to the ambient atmospheric pressure scale height H ($H = \frac{kT}{mg}$, where k is Boltzman constant, T is temperature, m is mass of abundant elements like nitrogen molecules and g is acceleration due to gravity; in the lowest 100 kms of the Earth's atmosphere, the scale height of variations is $\sim$10 km; see also http://www.atmos.colostate.edu/~davet/AT606/Chapters/CH01.pdf, Section 1.3.4, page 13), hence, the assumption that the terms "R, U, V, and W" are independent of altitude is reasonable.

With these adopted physical assumptions and by integrating on both sides with respect to z, the partial differential equation above can be converted into the following ordinary differential equation:

$$\frac{dP}{dt} = -\left(\frac{V+2U}{2z_0}\right)P - \frac{e^{z_0}}{2z_0^2}\left[-E_2V + (R-W)gB - g(R^2 - W^2) + U(E_1 - E_2) + z_0\frac{d^2}{dt^2}(R-W)\right], \tag{7}$$

where z_0 is vertical thickness of the clouds.

2.1. Description of the equation for the rate of precipitation

We would like to add that although it may appears that Indian summer monsoon rainfall is being explained by just one equation with two parameters (i.e., cloud and rain water mixing ratios) linked to sunspot and coronal forcing, but when one examines the equation closely, there are other equally important physical variables such as acceleration due to gravity '*g*' and temperature structure (that is represented as the dimensionless temperature ratio parameter, *B*, in the right hand side of Eq. (7)) of the ambient atmosphere that ultimately constrain the height of formation of clouds and hence rainfall. The importance of *g* can be gauged from Section 3 that, as *g* is related to the formation heights of cloud, if we change cloud height by a few meters, for example, from the canonical cloud height (~2 km) used in the simulations, the magnitude of simulated rainfall changes substantially compared to the observed Indian monsoon rainfall.

It is also to be noted that the single equation is derived from different moment equations that describe the physics of cloud and rainfall, so we argue that the true nature of our zero-order modeling attempt is more multi-dimensional and multi-variable constrained than it may first appear. The point here is that we have approached this classical problem of Indian monsoonal rainfall variation with a fresh and novel new approach that has never been performed nor attempted before, to the best of our knowledge.

Eq. (7) is similar to the equation of a forced harmonic oscillator for the rate of precipitation with *W* and *R* of the cloud as forcing variables. These forcing terms in the above equation are assumed to be functions of solar activity (combined effects of sunspot and coronal hole variabilities) that have sinusoidal variations of the forms $W = W_0\sum_i(\sin(\omega_i t) + \sin(\omega_i t + \theta))$ and $R = R_0\sum_i(\sin(\omega_i t) + \sin(\omega_i t + \theta))$, respectively (where W_0 and R_0 are constant amplitudes, t is a time variable, $\omega_i = \frac{2\pi}{T_i}$ are the well-known frequencies (periods T_i) observed in solar activity time series). In both *W* and *R*, the first forcing term is from sunspot activity while the second forcing term assumed to be from coronal hole variation (with a phase difference of θ in radians; observations show that sunspot and coronal hole activity occurrence indices have an opposite phase, that means when the sunspot's activity reaches maximum, coronal hole occurrence has a minimum activity). We considered the solar forcing to consist of periodicities ranging from daily, yearly to decadal-long timescales, *viz.*, $T_1 = 9$ days, $T_2 = 13$ days, $T_3 = 27$ days, $T_4 = 1.3$ years, $T_5 = 5$ years, $T_6 = 11$ years and $T_7 = 22$ years are considered. Such solar-activity periods have been reported and published in the literature (see Stenflo and Vogel, 1986; Pap et al., 1990; Hiremath, 2002; Krivova and Solanki, 2002; Nayar et al., 2002; Obridko and Shelting, 2007; Temmer et al., 2007; Hiremath, 2009b; Mendoza and Velasco-Herrera, 2011; Weng, 2012a; Katsavrias et al., 2012 and references therein), so we refer detailed discussions in those papers.

We wish to add that periods of the solar forcing are important factors that completely determine the amplitude of the simulated rainfall activity. For example, as described in Section 3, if those shorter solar periods are not taken into account in the simulations, we ended up with wrong precipitation values that are entirely different from the observed rainfall activity. We also appreciate and understand the extreme range of mean rainfalls among different affected monsoonal regions, but we recall that our modeling effort is one of "global"-scale (i.e., aggregated over the full geographical extents of the Indian monsoon region) study.

3. Solutions of the equation of rate of precipitation and results

3.1. Solutions without the effect of aerosols

One can notice that the equation for rate of precipitation (Eq. 7) is mainly derived from macrophysical equations. In addition, for the following two reasons and as a first approximation, we neglect the details of microphysics of the clouds in this simulation. First of all, we do not have reliable information of microphysical parameters (such as density, natural or anthropogenic aerosols, *etc.*) and their long term variations, especially on decade to century scales. Secondly, time scales (~years) involved in our parameterized processes are greater than the time scales of microphysics (~minutes-to-hours). For example, if one perturbs the tropospheric density structure, acoustic-gravity waves with periods ~10 min (Pierce and Coroniti, 1966) are created and may affect the cloud structure and hence the formation of precipitation as well. Hence, by neglecting clouds' microphysics and further simplifying a complex monsoon system, we assume that precipitation is created by evolving Eq. (7) and then we may probe further as to how the long-term monsoonal rainfall variability could be modulated by solar activity as an external forcing on the Earth's coupled land-atmosphere–ocean system.

Assuming that clouds are situated at an altitude of around 2 km (e.g., Manohar et al., 2001 showed that optimal altitudes for cloud formation around Pune are about 1.75–1.9 km) and starting from 1850 onwards, by giving different physical initial conditions (see Fig. 1) and as an initial value problem, Eq. (7) is numerically solved (the IDL routine, fifth-order Runge–Kutta–Verner scheme is adopted) to get the rate of precipitation for each day. These daily simulated precipitation values are then averaged over months and the aggregate summer (June–September) monsoon rainfall for each year is ultimately computed. The different initial conditions (in MKS units) for the rate of precipitation *P*, cloud's rain (*R*) and water (*W*) mixing ratios, acceleration due to gravity *g*, the dimensionless temperature ratio *B*, thickness of the cloud z_0, effective fall (*V*) and vertical (*U*) velocities, cloud evaporation or condensation (E_1) and rate of evaporation (E_2), respectively, are presented in Table 1. In addition, goodness of fit χ^2 (small value suggests that the fit is good) between the simulated and measured Indian summer monsoon rainfall is also given in that table.

A small value of χ^2 suggests that the observed and simulated rainfall are not different statistically. To be more specific, in order that simulated results are as close to the observed results, the computed χ^2 should be less than 162 (for the $\chi^2_{0.05}$) and 175 (for the $\chi^2_{0.01}$), respectively. If one examines the last two columns of Table 1, χ^2 values (of 321 and 201; when the effect of sunspot alone is considered) for both Parthasarathy and Sontakke data are higher than $\chi^2_{0.05}$ and $\chi^2_{0.01}$ criteria. In this case, the null hypothesis has to be rejected. Whereas when we consider the combined effect of both the sunspot and the coronal hole activity, we get the χ^2 (~7 for Parthasarathy's data and ~11 for Sontakke's data) that are far less than $\chi^2_{0.05}$ and $\chi^2_{0.01}$ values. Hence, for both the combined sunspot and coronal activities, we accept (or cannot reject) the null hypothesis (that observed and simulated values commensurate with each other). Thus, it is reasonable to propose that when studying the co-relationship between Indian monsoon rainfall and the solar activity in the future, one should not consider the sunspot activity alone as adopted in previous studies (e.g., Hiremath and Mandi, 2004 and references therein).

Different columns in Table 1 are: (i) first column-different physical parameters, (ii) second column-magnitudes (in SI units) of different initial conditions, (iii) third and fourth columns-χ^2 value for

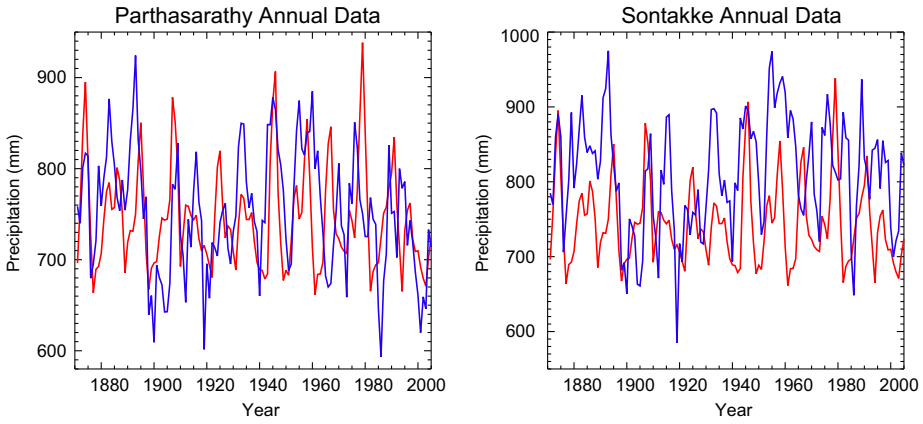

Fig. 1. Result on the left panel compares the computed (red curve) annual rate of precipitation variability to the smoothed observed (blue curve) yearly homogeneous Indian summer monsoon rainfall (sum over all the four monsoonal rainy months of June-September) variability data (i.e., so-called "Parthasarathy" record obtained from the Indian Institute of Tropical Meteorology; the website is maintained by Rupa Kumar and colleagues, see Hiremath and Mandi (2004) for details of the data set) for the 1871 to 2005 interval. The simulated precipitation presented on the right panel is the same as left panel but the observed (combined data of North West and Peninsular India) rainfall is taken from Sontakke et al., 2008 (also obtained from the Indian Institute of Tropical Meteorology website). Error bar ($=\sigma/(n)^{1/2}$, where σ is standard deviation and n is number of 4 monthly points of the June-September rainfall) of the observed rainfall is computed from the summer monsoon rainfall data and those error bars are not shown on the figure in order to avoid the excessive crowding of data points and time series. The maximum values of the measurement error bars for two observational data sets are 48 mm and 53 mm, respectively. (For interpretation of the references to color in this figure legend, the reader is referred to the web version of this article.)

Table 1
Different initial parameters used for the numerical solutions for the rate of precipitation equation.

Different initial parameters	Values (in SI units)	χ^2_{spot}	$\chi^2_{spot+ch}$
Rate of precipitation (P)	10.0		
Clouds rain (R)	0.5		
Water mixing ratio (W)	6.5		
Acceleration due to gravity (at 2 km height)	−9.79		
Dimensionless temperature ratio (B)	−1.0	320.612[a]	6.955[a]
Thickness of the cloud (z_0)	0.9	201.230[b]	11.418[b]
Effective fall velocity (V)	1.5		
Vertical velocity (U)	1.2		
Cloud evaporation ($E1$)	−0.5		
Rate of evaporation ($E2$)	2.0		
Phase difference θ (radians)	1.57		

[a] Value of χ^2 for Parthasarathy's Rainfall Data.
[b] Value of χ^2 for Sontakke's Rainfall Data.

both solutions including the solar effects with sunspot alone and with the combined sunspot and coronal holes index.

In order to match with the real summer monsoon rainfall data that starts from 1871 onwards, we find that simulated summer monsoon rainfall best matches (and has best fit with minimum value of χ^2) the real-world data if we adopt a time lag of 7 years. This result is reasonable as the Earth climatic system's response is more likely a non-linear, rather than linear, function of solar activity forcing (Weng, 2012b). Moreover, as various statistical studies (Hiremath and Mandi, 2004) suggest that solar activity leads (by ~1.5 years) Indian monsoonal rainfall variability, it is not surprising that such a simulated rainfall variability also yields a similar time lag. Importantly, we find that both the amplitude and annual-mean variability of the simulated rainfall time series changes drastically if one changes any of the local cloud-related parameters slightly (*viz.*, the cloud and water vapor mixing ratios W and R, acceleration due to gravity g and, altitude and thickness of the clouds z_0) through the external forcing parameterization (due to phase difference θ between the sunspot and coronal hole activities).

In order to test the importance of forcing due to different solar periods on the simulated precipitation, we used different combination (starting with only two solar periods to the inclusion of all seven periods) of the periods. It is found that, with the same physical initial conditions, the simulated precipitation time series can fully capture the variabilities (amplitude and temporal) of the real rainfall data *only if* all the seven periods (9, 13 and 27 days; 1.3, 5, 11 and 22 years) are included. Another physical clue from our sensitivity experiments is that the inclusions of the shorter solar periods can be shown to be more important in emulating the dynamical evolution of the observed Indian summer monsoon rainfall than the longer ones.

It is relevant to note from Figs. 1–3 that, even with all the aforementioned assumptions and approximations, the simulated precipitation variability indeed matches the observed Indian monsoon rainfall variability rather well. In Fig. 1, the left panel illustrates, the simulated (red curve) and observed (blue curve) homogeneous rainfall data (as compiled by Parthasarathy et al. (1993)). The right panel of Fig. 1 shows the same simulated (red) with the observed (blue) rainfall data as compiled by Sontakke et al. (2008). Note that there is the overall similarity of the simulated rainfall results with both the observed rainfall data sets, although there is a slightly larger variance between our simulated and Sontakke's rainfall data. This variance is possibly due to less rainfall area coverage in Sontakke's data record (i.e., we have considered Sontakke's combined data from Northwest India and Peninsular India) when compared to the larger area coverage in Parthasarathy's homogeneous rainfall data.

The results presented in Fig. 2 are essentially the same as Fig. 1 except that we added the simulated results of rainfall activity due to effect of sunspot alone (green curve). This is to contrast with the better results adopting both sunspot and coronal hole activity variations as the solar forcing parameter. Moreover, in Fig. 2, the magnitude of simulated rainfall value, adopting only sunspot forcing parameter, is ~1400 mm and that is roughly two times the observed average rainfall value of ~800 mm (see the green curve versus the blue curve in Fig. 2). On other hand, for the same initial conditions, the magnitude of simulated value of rainfall (see Fig. 1 or in Fig. 2, simulated rainfall represented by the lower red curve over plotted on the observed rainfall represented by the blue curve) for the combined effect sunspot and coronal hole is almost same as the average rainfall value of ~800 mm. In addition, the computed χ^2 value for both the combined effect of sunspot and coronal hole activity is very low (Table 1, ~7 for Parthasarathy's

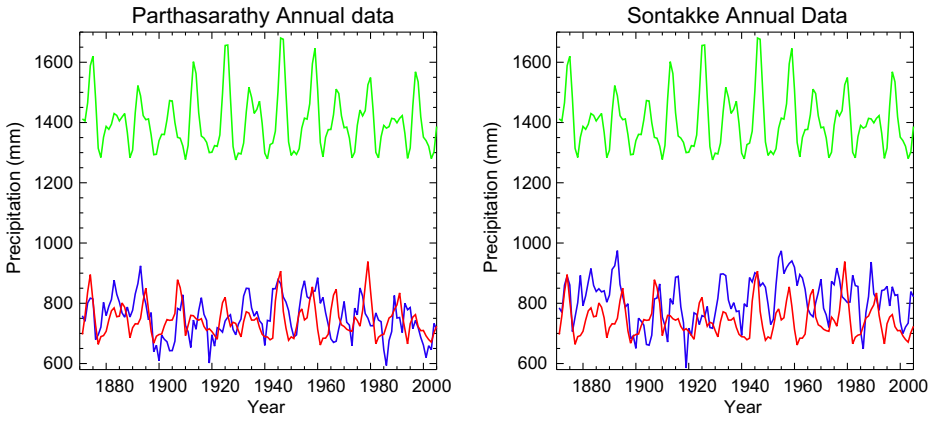

Fig. 2. Similar results as in Fig. 1. But, the simulated annual precipitation series adopted using only the sunspot series (green curves) as the solar activity forcing variable is also over plotted. This is to illustrate the superiority of the simulated rainfalls adopting both sunspot and coronal hole information (red curves). (For interpretation of the references to color in this figure legend, the reader is referred to the web version of this article.)

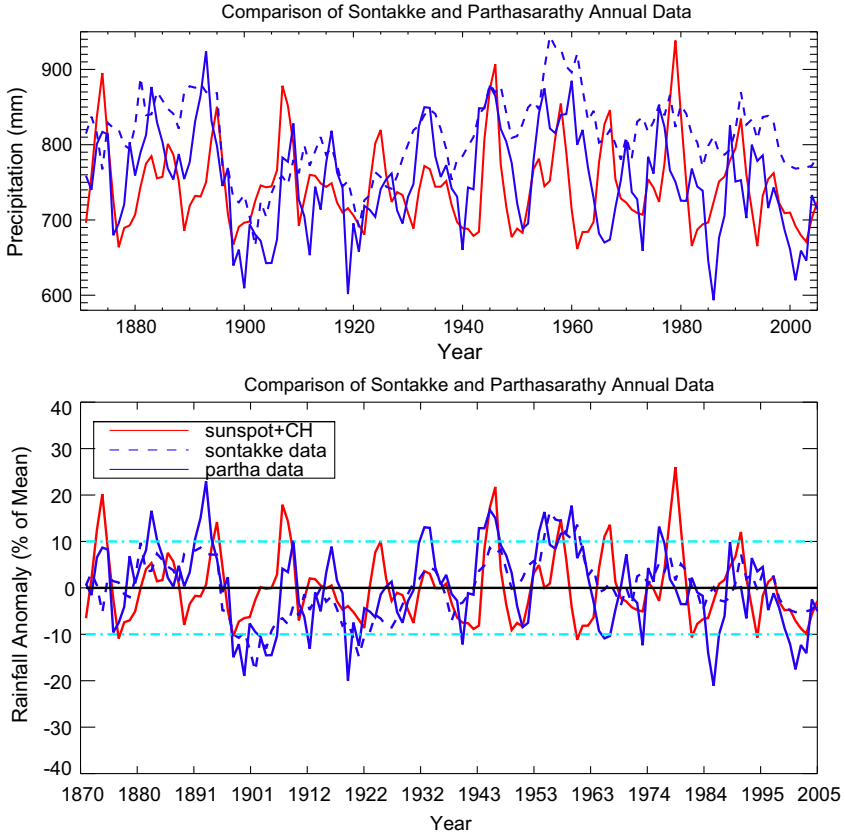

Fig. 3. Top panel: Same as Figs. 1 and 2, but both Parthasarathy's and Sontakke's data are over plotted on the simulated monsoon rainfall. The maximum values of the measurement error bars, not shown on the figure in order to avoid excessive crowding of data points, for both data sets are 48 mm and 53 mm, respectively. Bottom panel: Simulated and observed (both Parthasarathy and Sontakke) rainfall data from 1871 to 2005 plotted in percentage anomaly units also without the measurement error bars shown.

data and ~11 for Sontakke's data) that clearly tell the difference between green and red lines from the blue (observed) line.

For the years, 1871–2005, these results can also be more conveniently compared and contrasted by studying Fig. 3. In this figure, the top illustration represents simulated (red continuous line) versus two (blue continuous line for Parthasarathy data and blue dashed line for the Sontakke's data) observed rainfall variabilities. The bottom illustration represents the percentage anomaly of the simulated and both the observed rainfall data sets. From Fig. 3, it is also interesting to note that the optimal/best simulation of rainfall due to the combined solar activity index, without much of a numerical tuning of the variables involved in the precipitation equation, also simulated the extremes of rainfall activities causing floods and droughts similar to the observational records. In other words, the computed rainfall anomaly matches 90% (−10% to +10% of the mean value) of the anomaly of the observed rainfall data.

From all these results, we thus deduce that the most probable linkages between the solar and monsoon rainfall variabilities are through the solar activity modulation of the cloud water mixing

(W) and rain water mixing (R) ratios that are in turn presumed to co-vary with the two solar (sunspot and coronal hole) activity indices adopted.

Another important result from our study is that, while examining the relationship between the Indian monsoon rainfall and the solar variability, one should not consider only the sunspot numbers (as commonly assumed in almost all previous studies) as the external forcing parameter. Instead, one should also take into account the plausibly important effects of solar coronal hole activities (see the original discussion in Soon et al., 2000) that are also an important source of variability originated from our magnetic sun. The significant difference of the simulated rainfalls that adopted sunspot-only as the external solar driver when compared to the better simulated rainfall variability using the combined sunspot plus coronal hole activity index supports this interpretation (see the contrasting results in Fig. 2).

3.2. Solutions with the effect of aerosols

There are many studies that specialized and focused on the effect of aerosols on the Indian monsoon rainfall. In fact in one of our previous study (Hiremath, 2006b) on the sun-Indian monsoon relationship, some of variabilities of monsoon characteristics are interpreted as effects of aerosols on the rain forming clouds due to either intermittent source of sulfate aerosols from volcanic eruptions or due to intrusion of interstellar dust particles (e.g., Love and Brownlee, 1993; Yada et al., 2000; Lal and Jull, 2002) in the Earth's atmosphere. Whereas previous studies (Ramanathan et al., 2005; Meehl et al., 2008; Collier and Zhang, 2009; Gautam et al., 2009; Bollasina et al., 2011; Lau and Kim, 2010; Gadgil and Srinivasan, 2012; Sajani et al., 2012; Patil et al., 2013), focus mainly on the effect of anthropogenic aerosols, are suggesting that: (i) depending upon the physical conditions, precipitation either decreases or increases; (ii) indirectly aerosol heat the cloud and the ambient medium resulting in an increase of height of the precipitating clouds. These two proposed physical processes are now considered and studied in our simulations.

Although the effect of aerosol is clearly important on *in situ*, local and regional spatial scales, the key question is how much of the original precipitation will be altered when considering over the full spatial domain covered by the dynamic phenomenon of Indian monsoon. In order to arrive at an upper limit estimate of the total aerosol effects on Indian monsoonal rainfall change, we adopt the following calculations. According to the IPCC Fourth Assessment Report: *Climate Change 2007* (Fig. 7.22, http://www.ipcc.ch/publications_and_data/ar4/wg1/en/figure-7-22.html), it turns out that, on average, precipitation of the Northern Hemisphere is decreased by ~0.2 mm/day or ~6 mm/month when the total effect of anthropogenic aerosols are included in the computer climate model simulations. For the period from 1871 to 2005, if we consider the measured monthly average of Indian summer monsoon rainfall to be (~800 mm), then total percentage change for the monthly average is $((6/800) \times 100)$ ~0.7–1%. This is indeed a small relative percentage change induced by total anthropogenic aerosol forcing.

Assuming that aerosol forcing affects the precipitation, the term P in Eq. (7) is parameterized as $P = P_0 + P'$. Here P_0 is precipitation without the effect of aerosols and P' is precipitation due to aerosols. Further, from 1871 to 2005, we assumed time variation of P' under the following four scenarios: (i) linearly increasing trend, (ii) a non-linear increasing trend, (iii) linear decreasing trend and, (iv) non-linear decreasing trend. In addition, we consider radiative effects of aerosols to be indirectly contribute to heating the clouds and surrounding ambient temperatures. Hence, in our simulations the dimensionless temperature quantity, B, in Eq. (7) is considered to be of increasing (both the cases of linear and nonlinear) trend. For all these six scenarios and situations, we found that there is no substantial increase or decrease of overall Indian monsoonal rainfall either in terms of magnitude or temporal variability.

We, therefore, tentatively and cautiously conclude that the solar forcing effects are a far more important factor for the genesis and sustenance of Indian summer monsoon rainfall variations when compared to total aerosol effects as modeled by and shown in Fig. 7.22 of the IPCC 2007 report. Future modeling works must clearly study the combined effects of natural (for example sea salts), cosmic (due to intrusion of dust particles in the atmosphere) and anthropogenic aerosols and, influence of galactic cosmic rays (Rawal et al., 2013 and references there in) in affecting simulated rainfalls over individual spatial domains of the Indian monsoon phenomenon.

4. Discussion and conclusion

It is important to examine whether observations (either from ground or satellite data) show any association between the combined solar activity index and the parameterized cloud and rain water mixing ratios. As the cloud and rain water mixing ratios depend directly on the ambient atmospheric precipitable water vapor, a way for checking our original assumption is to look for any association between variabilities of atmospheric precipitable water vapor and the combined solar activity from past observations. In order to confirm or reject this reasoning, we used the Smithsonian Astrophysical Observatory (SAO) data of precipitable water vapor (Abbot et al., 1932; Abbot et al., 1942) (data is available at http://ftp.ngdc.noaa.gov/STP/SOLAR_DATA/SOLAR_IRRADIANCE/abbot/) for the historical period from 1923 through 1936. As the Indian monsoon rainfall activity may be related to Earth's global precipitation (Hiremath and Mandi, 2004), it is not unreasonable to consider the SAO data of atmospheric precipitable water. As the coronal hole data is not available during this period, by considering the observed empirical fact that sunspot activity lags the coronal hole activity by roughly 5 years (Bravo and Stewart, 1997), sunspot data that were shifted by 5 years back are considered as the proxy for historical coronal hole activity for 1923–1936 interval. That means for the present analysis, sunspot activity is considered for the years 1923–1936. Where as the sunspot data from 1918 to 1931 are treated as the proxy for coronal hole activity. As magnetic energy[1] is directly proportional to the square of number of sunspots, hence the summation of the square of sunspot and coronal hole activity numbers is treated as the combined solar activity.

The SAO's atmospheric precipitable water is obtained from the ratio of the intensity in three water–vapor absorption bands to the continuum intensity. From the daily data of precipitable water, monthly mean and its error ($=\frac{\sigma}{\sqrt{N}}$, where σ is standard deviation and N is number of data points during a month) are computed. In this way the raw data are corrected for any of the diurnal/seasonal changes, especially due to volcanic eruptions.

In Fig. 4, for a typical solar cycle 1923–1933, the monthly mean of atmospheric precipitable water (lagged by 10 months), solar UV irradiance, total solar irradiance (TSI) and combined solar activity

[1] If B is strength of magnetic field structure of the plasma, then according to magnetohydrodynamic phenomena, magnetic energy is defined as square of magnitude of magnetic field, i.e., $B^2/8\pi$ ergs. This relationship is basically derived from the Lorentzian Force ($J \times B$) of the magnetized plasma, where J is the current density parameter. Since sunspots have a strong (~10^3 Gauss) magnetic field strength, a typical sunspot whose area (A) is ~$10^{10} - 10^{18}$ cm^2, is likely to introduce magnetic energy $\left(\frac{B^2 A}{8\pi}\right) \sim 10^{15} - 10^{23}$ ergs of energy to the solar system environment. For example, solar flare is believed to be generated from the conversion of this magnetic energy into thermal and radiative energies.

data are presented. In Table 2, mean, standard deviation, correlation (between precipitable water and the three solar activity indices) and its significance are presented. As the Indian monsoon rainfall lags nearly by one year with solar activity (Hiremath and Mandi, 2004, see Section 3 and Fig. 3), we get a maximum correlation if the Earth's atmospheric precipitable variability is also lagged by nearly one year (10 months). It is to be noted that, similar to Feulner, 2011 work, if we examine the relationship between SAO precipitable water data without any time lag and with sunspot data alone, we do not find any statistical correlations at all. However, given a 10 months lag of precipitable water vapor and the combined solar activity (as defined above), we get very good and significant correlations. A similar results to those presented in Fig. 4 are further illustrated as scatter plots in Figs. 5 and 6. Results of two (linear and exponential) least-square fits between precipitable water and different solar activity indices are presented in Tables 3 and 4, respectively. In both of these tables, the first column represents different solar activity indices, the second-to-seventh columns represent two coefficients of least-square fits with their uncertainties and, the ratios of $|\delta A/A|$ and $|\delta B/B|$, respectively. Whereas the χ^2 values computed from different fits are presented in the last column. The results illustrated in Figs. 5 and 6 suggest that our combined sunspot and coronal hole activity index of solar activity is correlated with the observed atmospheric precipitable water records over the test interval of 1923–1936.

We find that the explained variances for the correlations between solar activity indices with the precipitable atmospheric water vapor are indeed quite low. Furthermore, we have to accept the important warnings from climatology literature that correlation coefficients (see Legates and McCabe, 1999; Legates and McCabe, 2013; Sabade et al., 2011) are bad evaluators of modeling fits. Even a 100% correlation does not mean that there is a *causal and physical relationship* between the two variables. Hence, in order to delineate the effects of different solar indices on the precipitable atmospheric water vapor, we evaluated another parameter, viz., whether estimated ratios of uncertainties in the ratios ($\frac{\delta A}{A}$ and $\frac{\delta B}{B}$) of coefficients from the least square fit decreases substantially from one model fit to another model fit. We found that indeed the fit value substantially decreases from assuming a linear relationship to a non-linear relationship. That is, if we assume a linear relationship, even the best fit (based on the minimum value of χ^2) for both the sunspot and coronal hole data yields (see Table 3 last row) 21% error in the ratio $\frac{\delta A}{A}$ and 33% in the ratio $\frac{\delta B}{B}$ for the linear least square fit. Whereas, for non-linear (exponential) least-square fit (see Table 4 last row), uncertainties in the same ratios are 4.8% and 30%, respectively. Hence, in spite of low value of correlation coefficient (although it is still statistically significant), based on these improvements of uncertainties in the ratios of coefficients, we conclude that there is a non-linear relationship between the atmospheric water vapor precipitation and solar activity.

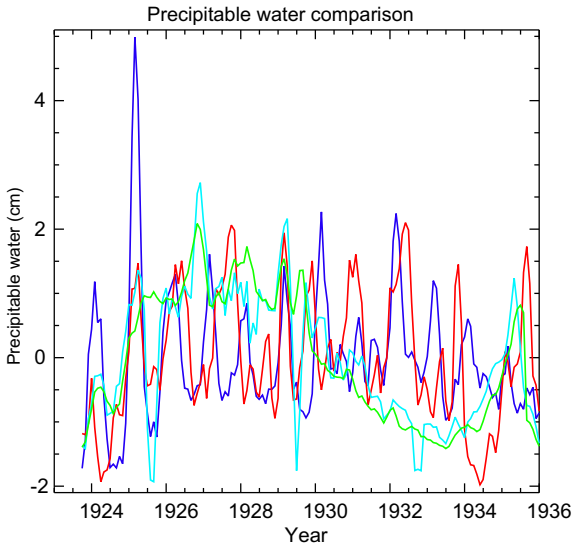

Fig. 4. Correlations between the smoothed, annual-averaged atmospheric precipitable water (blue continuous curve) and three measures of solar activity variations (red: the combined solar activity index, i.e, square of the sum of sunspot and coronal hole data series; green and indigo colors: solar UV and total [wavelength-integrated] solar irradiance [TSI] data, respectively, courtesy of Dr. J. Lean) for the 1923–1936 interval. The respective means and their standard deviations, correlation coefficients and their significance (small values suggest that the statistical correlations are not by chance) for the three solar activity time series are presented in Table 2. The maximum value of the measurement error bar for yearly atmospheric precipitable water is 3 cm. (For interpretation of the references to color in this figure legend, the reader is referred to the web version of this article.)

Our results are encouraging and unique in the sense that our proposed combined sunspot and coronal hole activity index also fare better (i.e., in different degrees of quantitative results) than corresponding correlations adopting the total solar irradiance and solar UV irradiance time series that were shared with us by Dr. J. Lean (see Tables 3 and 4 for the correlation coefficients of the three comparisons). Such a rare opportunity for checking, albeit important measurement uncertainties and instrumental limitations (see Hoyt, 1979), shows that our proposed use of the combined solar activity index for the study of sun-climate variability at least passes one independent, out of statistical samples, test.

Although beyond the scope of this study, let us digress and further interpret these interesting observational results. As the UV irradiance is attenuated at the stratospheric level (see e.g., Wang et al., 2013 for the strong coupling and non-linear interaction between the solar UV radiation and the highly reactive species like hydroxyl radical, OH, and ozone, O_3), it is obvious that the links between atmospheric precipitable water and the UV irradiance should be rather poorly correlated. Whereas the total irradiance, that enhances the water vapor and hence atmospheric precipitable water, reaches at the ground level and therefore the relationship between the atmospheric precipitable water with other two parameters (total irradiance and the combined solar activity) can be more closely related. It is also crucial and interesting to note from the results illustrated in Fig. 5 (i.e., TSI results at the upper right of Fig. 5): an increase of 0.1% of solar total irradiance from minimum activity to maximum activity increases the atmospheric precipitable water substantially (~200%). In other words, changes in the incoming solar radiation of ~1 W m^{-2} on the Earth's surface from one activity minimum to maximum results in increase of 200% precipitable water in the Earth's atmosphere. We suggest that this is one of the important results that answers the long-standing conundrum of any sun-climate relation (i.e., how the sun with merely 0.1% variation of radiation energy can have strong influences on the Earth's climate in general and Indian monsoon rainfall in particular). Thus, with a substantial increase of atmospheric precipitable water from solar minimum to maximum, we suggests that sun-climate and hence the solar activity and Indian monsoon rainfall relationship must physically be a non-linear phenomenon (see Weng, 2012a,b).

In order to substantiate this conjecture, for both the total irradiance and combined solar activity data with the atmospheric precipitable water is subjected to non-linear least square fit. To start with, polynomial fits of degree 2 and degree 3 are performed and it is found that both the fits are not good. Then the precipitable water with either total irradiance or combined solar activity data are subjected to exponential least square fit yielding a best fit compared to all the fits mentioned above. These results are illustrated in Table 4. One can notice from the last column of Tables 3 and 4 that values of χ^2 for all the fits are almost same. However, among

Table 2
Association of precipitable water with various solar activity indices.

Activity indices	Mean value	Standard deviation	Correlation coefficient	Significance
Precipitable water	43.8092 cm	14.0777 cm		
Ultraviolet emission	12.1670 W m^{-2}	0.030 W m^{-2}	0.0196	0.813
Irradiance	1365.82 W m^{-2}	0.197 W m^{-2}	0.2059	0.012
sunspot^2+CH^2	80.0846	15.397	0.2769	0.00065

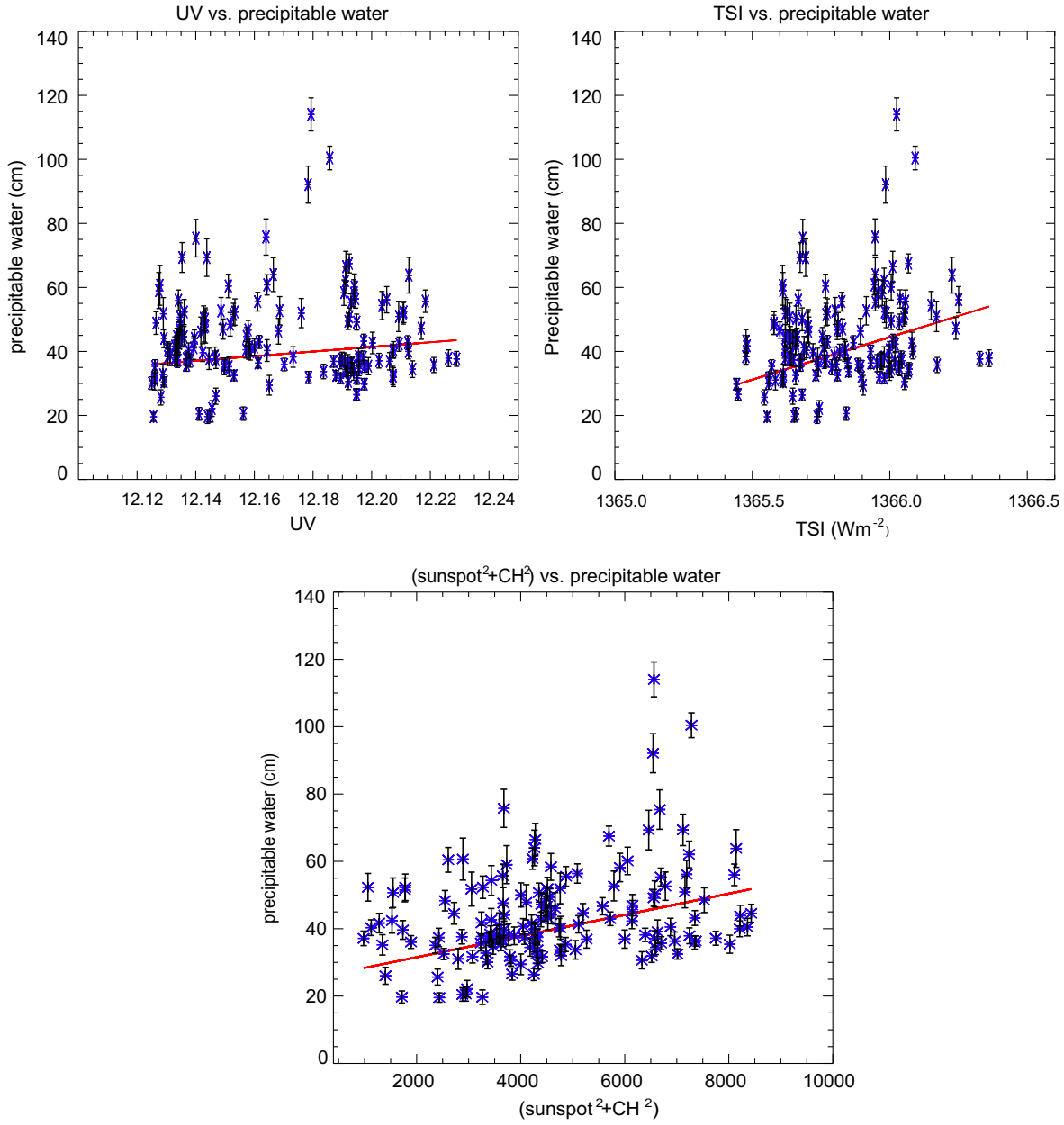

Fig. 5. Scatter plots illustrating monthly averaged atmospheric precipitable water versus solar UV irradiance, total (wavelength-integrated) solar irradiance and the combined sunspot and solar coronal hole index, respectively. The red continuous line in each plot represents the least square fit with a law of the form $Y = A + BX$ (where Y is precipitable water PW, X are the three dependent parameters listed above, A and B are constant coefficients that are determined from the least square fits). (For interpretation of the references to color in this figure legend, the reader is referred to the web version of this article.)

all the fits, percentage of uncertainty in both the ratios ($|\delta A/A|$ and $|\delta B/B|$) of coefficients A and B obtained from the exponential fit (i.e., the results in the right panel of Fig. 6, atmospheric precipitable water versus the combined solar activity) is a minimum. Considering this important fact, we conclude that non-linear least-square fit is slightly better when compared to the linear least square fit confirming our reasoning that sun-climate, especially sun-monsoon, relationship is a non-linear phenomenon.

We wish to add to the previously mentioned evidence of solar influence on the atmospheric precipitable water vapor based on

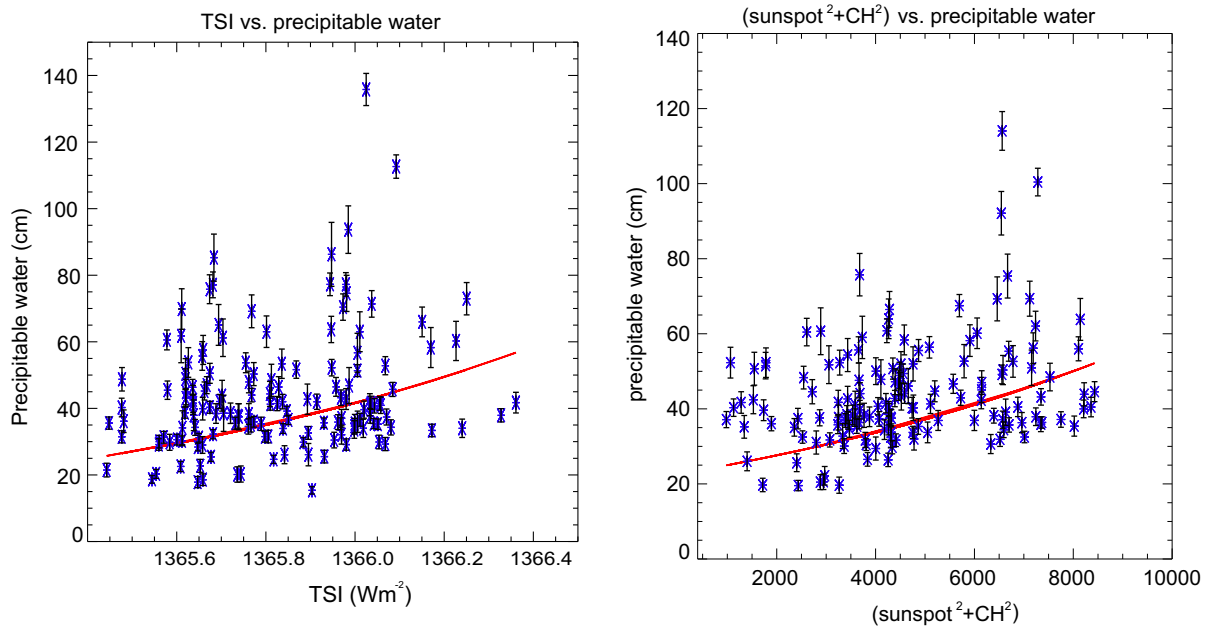

Fig. 6. Scatter plots illustrating monthly averaged atmospheric precipitable water versus total solar irradiance and the combined sunspot and solar coronal hole index, respectively, assuming non-linear relations. This is in contrast to the linear least-square fits shown in Fig. 5. The red continuous line in each plot represents the non-linear least square fit with a law of the form $Y = e^{(A+BX)}$ (where Y is precipitable water PW, X is either TSI or combined solar activity index, A and B are constant coefficients that are determined from the least square fits). Correlation coefficients are obtained by linearizing the exponential fits. (For interpretation of the references to color in this figure legend, the reader is referred to the web version of this article.)

Table 3
Least-square fits between precipitable water and solar activity indices assuming linear relations.

Activity indices	Coefficients obtained from linear fits						χ^2
	A	δA	$\lvert\delta A/A\rvert$	B	δB	$\lvert\delta B/B\rvert$	
Ultraviolet emission	−842.45	812.14	0.964	72.45	66.74	0.921	49.655
Total irradiance	−36262.81	13455.79	0.371	26.58	9.85	0.370	43.555
sunspot^2+CH^2	25.224	5.315	0.210	0.003	0.001	0.333	42.958

Table 4
Least-square fits between precipitable water and solar activity indices assuming nonlinear relations.

Activity indices	Coefficients obtained from exponential fits						χ^2
	A	δA	$\lvert\delta A/A\rvert$	B	δB	$\lvert\delta B/B\rvert$	
Total Irradiance	−1173.67	354.5	0.302	0.86	0.25	0.29	50.89
sunspot^2+CH^2	3.12	0.15	0.048	0.000099	0.00003	0.303	49.84

the new statistical and wavelet analyses by Maitra et al. (2014). Those authors find strong observational evidence of sun's influence on cloud liquid water content (LWC) and integrated water vapor (IWV) retrieved from the radiosonde data collected over nine different stations in India for the 1977–2012 interval. Hence, these observed results substantiate our hypotheses and simulations that cloud and rain water mixing ratios are among the most apparent physical linkages between the solar and Indian monsoon rainfall variabilities.

With the observed empirical sun-atmospheric precipitable water relationship, one should also expect a similar tendency in monsoon rainfall variability. From the previous study (Hiremath and Mandi, 2004; see Fig. 2), one can notice that there is a similar increasing trend ($\sim 20\%$) of monsoon rainfall activity from solar minimum to maximum although the increase in rainfall is not quantitatively as large of an increase as that of atmospheric precipitable water.

Although we have given some clues of sun-monsoon physical relationship in the introduction of the paper, in light of results from the derived precipitable equation and the strong empirical sun-atmospheric precipitable water relationship, we further refine the sun-monsoon causal relationship as follows. In general, main ingredients of formation of rainfall from the precipitable cloud are: (i) evaporation of water vapor from the Earth's land and water surfaces and oceans, (ii) microphysical quantities such as aerosols and formation of the clouds and, (iii) charged particles attached to seed particles in order to enhance the coalescence and condensation of water droplets leading to rainfall at a particular height of the atmosphere (see e.g., Manohar et al., 2001). In fact all these main and essential ingredients are inter-connected to the sun's time-varying activities. But we note that ingredient (i) seemed to have more obvious role in our zero-order modeling effort. Our interpretation and results are consistent with the findings by Lim et al. (2006) for tropical Atlantic.

Moreover and importantly, the monsoonal winds and the resulting rainfall are created and sustained by the temperature difference between the land and ocean masses that are heated by the sun. Although sun's total irradiance energy appears to be nearly

constant, even a small increase (decrease) ($\sim$1 W m^{-2}) at the ground level of the Earth on decadal time scale either enhances (decreases) the precipitation budget of the Earth. Hence, it is not surprising that majority of the droughts in the world occurred during the period of solar minimum when there is lesser amount of solar radiant energy to evaporate water vapor from the ocean and to maintain the strong circulation from the land-sea thermal contrast. One recent example is the severe drought due to failure of the Indian summer monsoon during 2009 and subsequent years.

To conclude this study, we have successfully simulated the historical Indian summer monsoon rainfall from 1871 through 2005 adopting the combined solar magnetic activity index which includes both the sunspot and coronal hole activity records. The simulations of the interannual to decadal variations are found to be sufficiently satisfactory and impressive enough to add weights to the great difficulties in rejecting any solar-monsoonal statistical correlation on such timescales. Our parametric modeling study proffers a useful step towards the ultimate identification and diagnosis of the physically relevant solar and hydrological quantities involved. Specifically, we suggest that the most probable linkages between solar magnetic variable outputs and Indian monsoon rainfall variabilities are through the solar activity modulation of the cloud water (W) and rain water mixing (R) ratios. Our simulations also argue for the importance of including coronal hole variability in any physical study of solar-Indian monsoon rainfall connection since the sole representation of solar magnetic variability using sunspot record alone is only a necessary but not a sufficient boundary condition.

Acknowledgments

This research has been carried out under "CAWSES India Phase-II program of Theme 1" sponsored by Indian Space Research Organization (ISRO), Government of India. We are grateful to both Professor Peter Conti, the editor and, the referee for useful and helpful comments that improved this manuscript substantially.

References

Abbot, C.G., Aldrich, L.B., Fowle, F.E., 1932. Annals of the Astrophysical Observatory of the Smithsonian Institution, vol. 5. p. 1.
Abbot, C.G., Aldrich, L.B., Hoover, W.H., 1942. Annals of the Astrophysical Observatory of the Smithsonian Institution, vol. 6. pp. 1–201.
Ananthakrishnan, R., Parthasarathy, B., 1984. J. Climatol. 4, 149.
Agnihotri, R., Dutta, K., Bhushan, R., Somayajulu, B.L.K., 2002. Earth Planet. Sci. Lett. 198, 521.
Agnihotri, R., Dutta, K., 2003. Curr. Sci. 85, 459.
Agnihotri, R., Dutta, K., Soon, W., 2011. J. Atmos. Sol. Terr. Phys. 73, 1980.
Badruddin, Singh, Y.P., Singh, M., 2006. In Proceedings of ILWS Goa workshop, Editors: N. Gopalswamy and A. Bhattacharya, 444.
Bhalme, H.N., Mooley, D.A., 1980. Mon. Weather Rev. 108, 1197.
Bollasina, M.A., Ming, Y., Ramaswamy, V., 2011. Science 334, 502.
Bravo, S., Stewart, G.A., 1997. Sol. Phys. 173, 193.
Choi, Y., Moon, Y.-J., Choi, S., Baek, J.-H., Kim, S.S., Cho, K.-S., Choe, G.S., 2009. Sol. Phys. 254, 311.
Claud, C., Duchiron, B., Terray, P., 2008. J. Geophys. Res. 113, D09105.
Collier, J.C., Zhang, G.J., 2009. Clim. Dyn. 32, 313.
Cranmer, S.R., 2009. Living Rev. Sol. Phys. 6, 3.
DelSole, T., Shukla, J., 2012. Geophys. Res. Lett. 39, L09703.
Feulner, G., 2011. Atmos. Chem. Phys 11, 3291.
Gadgil, S., Vinayachandran, P.N., Francis, P.A., Gadgil, S., 2004. Geophys. Res. Lett. 31, L12213.
Gadgil, S., Srinivasan, J., 2012. Curr. Sci. 103, 257.
Gautam, R., Hsu, N.C., Lau, K.-M., Kafatos, M., 2009. Ann. Geophys. 27, 3691.
Gray, L.J., Beer, J., Geller, M., Haigh, J.D., Lockwood, M., Matthes, K., Cubasch, U., Fleitmann, D., Harrison, G., Hood, L., Luterbacher, J., Meehl, G.A., Shindell, D., van Geel, B., White, W., 2010. Rev. Geophys. 48, RG4001.
Gupta, A.K., Das, M., Anderson, D.M., 2005. Geophys. Res. Lett. 32, L17703.
Higginson, M.J., Altabet, M.A., Wincze, L., Herbert, T.D., Murray, D.W., 2004. Paleoceanography 19, PA3015.
Hiremath, K.M., 2002. ESA Publications Division, ISBN 92-9092-815-8, 425, Ed. H. Sawaya-Lacoste.
Hiremath, K.M., Mandi, P.I., 2004. New Astron. 9, 651.
Hiremath, K.M., 2006a. In: Gopalswamy, N., Bhattacharyya, A. (Ed.), Proceedings of the ILWS Workshop, February 19, Goa, India. pp. 178–181.
Hiremath, K.M., 2006b. J. Astrophys. Astron. 27, 367.
Hiremath, K.M., 2009a. Sun Geosphere 4, 16.
Hiremath, K.M., 2009b. Available from arXiv:0909.4376.
Hiremath, K.M., 2010. Sun Geosphere 5, 17.
Hiremath, K.M., 2013. In: New Trends in Atomic and Molecular Physics. In: Springer Series on Atomic, Optical, and Plasma Physics, vol. 76. p. 317.
Hiremath, K.M., Hegde, M., 2013. Astrophys. J. 763, 137.
Hoyt, D.V., 1979. Rev. Geophys. Space Phys. 17, 427.
Johnson, R.H., Houze, R.A., Jr., 1987. In: Chang, C.-P., Krishnamurti, T.N. (Eds.), Monsoon Meteorology. p. 298.
Kailas, V.S., Narasimha, R., 2000. Curr. Sci. 78, 592.
Katsavrias, C., Preka-Papadema, P., Moussas, X., 2012. Sol. Phys. 280, 623.
Kerr, R.A., 2005. Science 308, 787.
Knudsen, M.F., Jacobsen, B.H., Riisager, P., Olsen, J., Seidenkrantz, M.S., 2012. Holocene 22, 597.
Kodera, K., Coughlin, K., Arakawa, O., 2007. Geophys. Res. Lett. 34, L03710.
Kripalani, R.H., Oh, J.H., Kulkarni, A., Sabade, S.S., Chaudhari, H.S., 2007. Theor. Appl. Climatol. 90, 133.
Krishnan, R., Choudhury, A.D., Chattopadhyay, R., Mujumdar, M., 2012. In: Tyagi, A. et al. (Eds.), Monsoon Monograph, vol. 2. p. 189. Available from <http://www.imd.gov.in/section/nhac/dynamic/Monsoonframe.htm>.
Krishnamurty, V., Shukla, J., 2012. In: Tyagi, A. et al. (Eds.), Monsoon Monograph, vol. 2. p. 266. Available from <http://www.imd.gov.in/section/nhac/dynamic/Monsoonframe.htm>.
Krivova, N.A., Solanki, S.K., 2002. Astron. Astrophys. 394, 701.
Lal, D., Jull, A.J.T., 2002. Astrophys. J. 576, 1090.
Lau, W.K.M., Kim, K.-M., 2010. Geophys. Res. Lett. 37, L16705.
Legates, D.R., McCabe Jr., G.J., 1999. Water Resour. Res. 35 (1), 233.
Legates, D.R., McCabe Jr., G.J., 2013. Int. J. Climatol. 33 (4), 1053.
Lei, J., Thayer, J.P., Forbes, J.M., Sutton, E.K., Nerem, R.S., 2008. Geophys. Res. Lett. 35, L10109.
Lim, G.-H., Suh, Y.-C., Kim, B.-K., 2006. Q. J. R. Meteorolog. Soc. 132, 1139.
Love, S.G., Brownlee, D.E., 1993. Science 262, 550.
Ma, L., Han, Y., Yin, Z., 2007. Appl. Geophys. 4, 231.
Maitra, A., Saha, U., Adhikari, A., 2014. Physics. http://dx.doi.org/10.1016/j.jastp.2014.06.010.
Mannucci, A.J., Tsurutani, B.T., Solomon, S.C., Verkhoglyadova, O.P., Thayer, J.P., 2012. Trans. Am. Geophys. Union 93, 77.
Manohar, G.K., Kandalgaonkar, S.S., Tinmaker, M.I.R., 2001. Curr. Sci. 80, 555.
Meehl, G.A., Arblaster, J.M., Collins, W.D., 2008. J. Clim. 21, 2869.
Meehl, G.A., Arblaster, J.M., Matthes, K., Sassi, F., van Loon, H., 2009. Science 325, 1114.
Mendoza, B., Velasco-Herrera, V.M., 2011. Sol. Phys. 271, 169.
Neff, U., Burns, S.J., Mangini, A., Mudelsee, M., Fleitmann, D., Matter, A., 2001. Nature 411, 290.
Nigam, R., Khare, N., Nair, R.R., 1995. J. Coastal Res. 11, 1099.
Obridko, V.N., Shelting, B.D., 2007. Adv. Space Res. 40, 1006.
Pap, J., Bouwer, S.D., Tobiska, W.K., 1990. Sol. Phys. 129, 165.
Parthasarathy, B., Kumar, K.R., Munot, A.A., 1993. Proc. Indian Acad. Sci. Earth Planet. Sci. 102, 121.
Patil, S.D., Preethi, B., Bansod, S.D., Singh, H.N., Revadekar, J.V., Munot, A.A., 2013. J. Atmos. Sol. Terr. Phys. 102, 1.
Perry, C.A., 2007. Adv. Space Res. 40, 353.
Pierce, A.D., Coroniti, S.C.A., 1966. Nature 210, 1209.
Prabha, Thara V., Khain, A., Maheshkumar, R.S., Pandithurai, G., Kulkarni, J.R., Konwar, M., Goswami, B.N., 2011. J. Atmos. Sci. 68, 1882.
Prabhakaran Nayar, S.R., Radhika, V.N., Revathy, K., Ramadas, V., 2002. Sol. Phys. 208, 359.
Preethi, B., Kripalani, R.H., Krishna Kumar, K., 2010. Clim. Dyn. 35, 1521.
Rajeevan, M., Unnikrishnan, C.K., Preethi, B., 2012. Clim. Dyn. 38, 2257.
Ram, S.T., Liu, C.H., Su, S.-Y., 2010. J. Geophys. Res. 115, A12340.
Ramanathan, V., Chung, C., Kim, D., Bettge, T., Buja, L., Kiehl, J.T., Washington, W.M., Fu, Q., Sikka, D.R., Wild, M., 2005. Proc. Natl. Acad. Sci. USA 102, 5326.
Ramesh, R., Tiwari, M., Chakraborthy, S., Managave, S.R., Yadava, M.G., Sinha, D.K., 2010. Curr. Sci. 99, 1770.
Rawal, A., Tripathi, S.N., Michael, M., Srivastava, A.K., Harrison, R.G., 2013. J. Atmos. Sol. Terr. Phys. 102, 243.
Reddy, R.S., Neralla, V.R., Godson, W.L., 1989. Theor. Appl. Climatol. 39, 194.
Rogers, R.R. (Ed.), 1979. A Short Course in Cloud Physics, . second ed. Interna- tional series in Natural Philosophy second ed., 96 Pergamon Press, p. 202.
Sabade, S.S., Kulkarni, A., Kripalani, R.H., 2011. Theor. Appl. Climatol. 103, 543.
Sajani, S., Krishna Moorthy, K., Rajendran, K., Nanjundiah, R.S., 2012. J. Earth Syst. Sci. 121, 867.
Shugai, Yu.S., Veselovsky, I.S., Trichtchenko, L.D., 2009. Geomag. Aeron. 49, 415.
Sojka, J.J., McPherron, R.L., van Eyken, A.P., Nicolls, M.J., Heinselman, C.J., Kelly, J.D., 2009. Geophys. Res. Lett. 36, L19105.
Sontakke, N.A., Singh, H.N., Singh, N., 2008. ISSN 0252–1075, Contribution from IITM Research Report No. RR-121.
Soon, W., Baliunas, S., Posmentier, E.S., Okeke, P., 2000. New Astron. 4, 563.
Soon, W., Legates, D.R., 2013. J. Atmos. Sol. Terr. Phys. 93, 45.
Soon, W., Velasco-Herrera, V.M., Selvaraj, K., Traversi, R., Usoskin, I., Chen, C.-T.A., Lou, J.-Y., Kao, S.-J., Carter, R.M., Pipin, V., Severi, M., Becagli, S., 2014. Earth Sci. Rev. 134, 1.
Srivastava, R.C., 1967. J. Atmos. Sci. 24, 36.

Stenflo, J.O., Vogel, M., 1986. Nature 319, 285.
Sykora, J., Badalyan, O.G., Obridko, V.N., 2000. In: Wilson, A. (Ed.), Proceedings of the 1st Solar and Space Weather Euroconference, ESA SP, vol. 463. ESA Publications Division, Noordwijk, Netherlands, p. 680, 95.
Temmer, M., Vrsnak, B., Veronig, A.M., 2007. Sol. Phys. 241, 371.
Thamban, M., Kawahata, H., Rao, V.P., 2007. J. Oceanogr. 63, 1009.
Tiwari, M., Ramesh, R., Somayajulu, B.L.K., Jull, A.J.T., Burr, G.S., 2005. Curr. Sci. 89, 1583.
van Loon, H., Meehl, G.A., Arblaster, J.M., 2004. J. Atmos. Sol. Terr. Phys. 66, 1767.
van Loon, H., Meehl, G.A., 2012. Geophys. Res. Lett. 39, L13701.
Verbanac, G., Vršnak, B., Veronig, A., Temmer, M., 2011. Astron. Astrophys. 526, A20.
Vines, R.G., 1986. Int. J. Climatol. 6, 135.
Wang, S.-Y., Buckley, B.M., Yoon, J.-H., Fosu, B., 2013. J. Geophys. Res. Atmos. 118, 4373.
Wang, Y.J., Cheng, H., Edwards, R.L., He, Y., Kong, X., An, Z., Wu, J., Kelly, M.J., Dykoski, C.A., Li, X., 2005. Science 308, 854.
Wang, Y.-M., 2009. Space Sci. Rev. 144, 383.
Weng, H., 2012a. Adv. Atmos. Sci. 29, 867.
Weng, H., 2012b. Adv. Atmos. Sci. 29, 887.
Wu, G.X., Liu, Y., Zhu, X., Li, W., Ren, R., Duan, A., Liang, X., 2009. Ann. Geophys. 27, 3631.
Yada, T., Nakamura, T., Noguchi, T., Yano, H., Terada, K., Murakami, T., Kojima, H., Japanese Amm Working Group, 2000. Meteorit. Planet. Sci. 35 (Suppl.), A173.
Yadava, M.G., Ramesh, R., 2007. New Astron. 12, 544.